

# Pvr and distinct downstream signaling factors are required for hemocyte spreading and epidermal wound closure at *Drosophila* larval wound sites

Chang-Ru Tsai,<sup>1,2,†</sup> Yan Wang,<sup>2</sup> Alec Jacobson,<sup>2,‡</sup> Niki Sankoorikkal,<sup>2,§</sup> Josue D. Chirinos,<sup>2,††</sup> Sirisha Burra,<sup>2,‡‡</sup> Nishanth Makthal,<sup>3</sup> Muthiah Kumaraswami,<sup>3</sup> and Michael J. Galko<sup>1,2,4,\*</sup>

<sup>1</sup>Program in Developmental Biology, Baylor College of Medicine, Houston, TX 77030, USA

<sup>2</sup>Department of Genetics, University of Texas MD Anderson Cancer Center, Houston, TX 77030, USA

<sup>3</sup>Department of Pathology and Genomic Medicine, Houston Methodist Hospital, Houston, TX 77030, USA and

<sup>4</sup>Genetics & Epigenetics Graduate Program, University of Texas MD Anderson Cancer Center, Houston, TX 77030, USA

\*Corresponding author: Department of Genetics- Unit 1010, University of Texas MD Anderson Cancer Center, 1515 Holcombe Blvd, Houston, TX 77030, USA.

Email: mjgalko@mdanderson.org

<sup>†</sup>Present address: Department of Molecular Physiology and Biophysics, Baylor College of Medicine, Houston, TX 77030, USA.

<sup>‡</sup>Present address: Carleton College, Northfield, MN 55057, USA.

<sup>§</sup>Present address: School of Medicine, Texas Tech University Health Sciences Center, Lubbock, TX 79430, USA.

<sup>††</sup>Present address: Harvard Medical School, Boston, MA 02115, USA.

<sup>‡‡</sup>Present address: Department of Melanoma Medical Oncology, University of Texas MD Anderson Cancer Center, Houston, TX 77030, USA.

## Abstract

Tissue injury is typically accompanied by inflammation. In *Drosophila melanogaster* larvae, wound-induced inflammation involves adhesive capture of hemocytes at the wound surface followed by hemocyte spreading to assume a flat, lamellar morphology. The factors that mediate this cell spreading at the wound site are not known. Here, we discover a role for the platelet-derived growth factor/vascular endothelial growth factor-related receptor (Pvr) and its ligand, Pvf1, in blood cell spreading at the wound site. Pvr and Pvf1 are required for *spreading in vivo* and in an *in vitro* spreading assay where spreading can be directly induced by Pvf1 application or by constitutive Pvr activation. In an effort to identify factors that act downstream of Pvr, we performed a genetic screen in which select candidates were tested to determine if they could suppress the lethality of Pvr overexpression in the larval epidermis. Some of the suppressors identified are required for epidermal wound closure (WC), another Pvr-mediated wound response, some are required for hemocyte spreading *in vitro*, and some are required for both. One of the downstream factors, Mask, is also required for efficient wound-induced hemocyte spreading *in vivo*. Our data reveal that Pvr signaling is required for wound responses in hemocytes (cell spreading) and defines distinct downstream signaling factors that are required for either epidermal WC or hemocyte spreading.

**Keywords:** inflammation; larvae; cell-spreading; Pvr; hemocytes; *Drosophila*; wound closure

## Introduction

*Drosophila* larvae have emerged as a useful system to study tissue repair responses (Tsai et al. 2018), including wound closure (WC) (Galko and Krasnow 2004; Baek et al. 2010; Kakanj et al. 2016), epidermal cell–cell fusion (Wang et al. 2015; Lee et al. 2017), and basement membrane dynamics (Ramos-Lewis et al. 2018). Following injury, larval barrier epithelial cells at the wound edge locally detach from the apical cuticle and migrate into the wound gap. This process requires both JNK signaling (Galko and Krasnow 2004; Lesch et al. 2010; Lee et al. 2019) and Pvr signaling (Wu et al. 2009). The latter is required in some manner for epithelial extension into the wound site, though it has been difficult to identify downstream genes of this pathway given a lack of pathway reporters that function well *in vivo* during the larval stage.

*Drosophila* is also a good system for studying damage-induced inflammatory responses (Brock et al. 2008; Stramer and Dionne 2014). Hemocyte responses to wounding in *Drosophila* are remarkably stage-specific. The recruitment of hemocytes to wounds during the nonlocomotory embryonic (Stramer et al. 2005) and pupal stages (Moreira et al. 2011) is primarily through directed cell migration of hemocytes. These migrations require hydrogen peroxide (Moreira et al. 2010) and likely other cues (Weavers et al. 2016). Larvae, which are a locomotory foraging stage that follows embryogenesis and precedes pupariation, have a different mechanism of recruiting hemocytes to damaged tissue. In larvae, circulating hemocytes patrol the open body cavity and adhere to damaged tissue if they encounter it (Babcock et al. 2008). Once at the wound, attached hemocytes spread, change from an approximately spherical to a flattened fan-like morphology, and

Received: June 10, 2021. Accepted: October 12, 2021

© The Author(s) 2021. Published by Oxford University Press on behalf of Genetics Society of America.

This is an Open Access article distributed under the terms of the Creative Commons Attribution License (<https://creativecommons.org/licenses/by/4.0/>), which permits unrestricted reuse, distribution, and reproduction in any medium, provided the original work is properly cited.

phagocytose cell debris. At the larval stage, even hemocytes close to the wound do not respond to it through directed migration (Babcock et al. 2008). Some hints about the molecules required for blood cell attachment have been gleaned from other insect species (Levin et al. 2005; Nardi et al. 2006) and from vertebrates (Eming et al. 2007). Likewise, some studies of *Drosophila* cell morphology have been performed in hemocyte-like cells in vitro (Kiger et al. 2003; D'Ambrosio and Vale 2010) and even in response to wounding in vivo (Kadandale et al. 2010). However, the molecules required for wound-induced spreading in vivo and their relationship to in vitro observations remain unclear.

Pvr is a *Drosophila* receptor tyrosine kinase (RTK) related to the vertebrate vascular endothelial growth factor (VEGF) receptor (Heino et al. 2001; Cho et al. 2002). Pvr controls a variety of developmental signaling events including hemocyte differentiation (Mondal et al. 2014), migration (Cho et al. 2002; Wood et al. 2006), and survival (Munier et al. 2002; Bruckner et al. 2004; Zettervall et al. 2004). Pvr is also required for epithelial developmental migrations (McDonald et al. 2003; Ishimaru et al. 2004; Harris et al. 2007; Garlena et al. 2015) and for epidermal WC at the larval stage (Wu et al. 2009). Because Pvr is an RTK it presumably connects to a fairly canonical RTK signaling pathway downstream and some studies have identified downstream players in certain contexts (McDonald et al. 2003; Jékely et al. 2005; Fernández-Espartero et al. 2013). Notably, however, reliable reporters for monitoring pathway activity in vivo have been difficult to come by for this pathway. An alternative approach to finding pathway components, one with prior success for analyzing RTK pathways is genetic modifier screening (Smith et al. 2002; Sullivan and Rubin 2002). Here, we took advantage of the lethality of Pvr overexpression in the larval epidermis (Wu et al. 2009) to design a suppressor screen that could, in theory, identify downstream signaling components in this tissue. We then cross-checked the suppressors identified by the screen to see if they were required for larval epidermal WC or for hemocyte spreading at wound sites. This strategy revealed both shared and distinct downstream components for Pvr signaling in mediating epidermal WC and hemocyte spreading.

## Materials and methods

### Genetics

*Drosophila* were reared on standard cornmeal medium under a 12-h light-dark cycle. All crosses were cultured at 25 °C unless indicated. *w*<sup>1118</sup> was used as a control strain. *Pvr*<sup>c02859</sup> is a hypomorphic allele (Cho et al. 2002; Wu et al. 2009). *Pvr*<sup>M104181</sup> (Venken et al. 2011), referred to as *Pvr*<sup>null</sup>, contains a splice acceptor and a stop cassette in an early Pvr intron which leads to truncation. *Pvf1*<sup>EP1624</sup>, here referred to as *Pvf1*<sup>null</sup>, is a null allele (Cho et al. 2002; Wu et al. 2009). *Pvf2*<sup>c06947</sup>, here referred to as *Pvf2*<sup>hyppo</sup>, is a hypomorphic allele (Cho et al. 2002). *Pvf3*<sup>M04168</sup>, here referred to as *Pvf3*<sup>null</sup>, contains a splice acceptor and a stop cassette in an early Pvf3 intron which leads to truncation (Venken et al. 2011).

The GAL4/UAS system was used to drive tissue-specific gene expression of transgenes under UAS control (Brand and Perrimon 1993). For larval hemocytes, *hemolectinΔ-Gal4* (*hmlΔ-Gal4*) was used (Sinenko and Mathey-Prevot 2004); for the embryonic and larval epidermis, *e22c-Gal4* was used (Lawrence et al. 1995); for the larval epidermis, *A58-Gal4* was used (Galko and Krasnow 2004). To increase Pvr expression or activation in specific tissues, various Gal4 drivers were crossed to either UAS-Pvr or UAS-*ΔPvr* (Duchek et al. 2001). For the hemocyte spreading assay, we used *hmlΔ-Gal4*, UAS-GFP or *hmlΔ-Gal4* (Sinenko and Mathey-Prevot 2004), UAS-lifect-GFP (Hatan et al. 2011), and UAS-CD4-TdTom

(Han et al. 2011). For visualizing WC, we used *e22c-Gal4*, UAS-*src-GFP*, UAS-*DsRed2-Nuc* or *A58-Gal4*, UAS-*src-GFP*, and UAS-*DsRed2Nuc* (Lesch et al. 2010). *e22c-Gal4*, UAS-*src-GFP*, UAS-*DsRed2Nuc*; *tubP-gal80<sup>ts</sup>* was used where temporal control of the Gal4/UAS system was needed (McGuire et al. 2004).

UAS-RNAi lines employed were: From Vienna *Drosophila* Research Center (Dietzl et al. 2007): KK108550 (MKK3<sup>RNAi#1</sup>), GD7546 (MKK3<sup>RNAi#2</sup>), KK100471 (CG1227<sup>RNAi</sup>), GD14375 (Pvr<sup>RNAi#1</sup>). Note: lines are listed as construct ID (GeneX<sup>RNAi</sup>). UAS-RNAi lines from the TriP Bloomington collection (Ni et al. 2011) were: JF01355 (*Luciferase*<sup>RNAi</sup>), JF02478 (*Ras*<sup>RNAi#2</sup>), HMS01294 (*Ras*<sup>RNAi#3</sup>), HMS01979 (*Vav*<sup>RNAi</sup>), HMS00173 (*Erk*<sup>RNAi</sup>), HMS05002 (MKK3<sup>RNAi#3</sup>), JF02770 (PI3K92E<sup>RNAi</sup>), HMS00007 (*Akt*<sup>RNAi</sup>), GL00156 (*Tor*<sup>RNAi#1</sup>), HMS00904 (*Tor*<sup>RNAi#2</sup>), JF02717 (*drk*<sup>RNAi</sup>), HMS01045 (*mask*<sup>RNAi</sup>), JF01792 (*Ck1α*<sup>RNAi#1</sup>), GL0021 (*Ck1α*<sup>RNAi#2</sup>), and GL00250 (*GckIII*<sup>RNAi</sup>). UAS-RNAi lines from NIG-Fly (<http://www.shigen.nig.ac.jp/fly/nigfly/index.jsp>; Accessed: 2021 November 15) were: 9375R-1 (*Ras85D*<sup>RNAi</sup>), 7717R-1 (MEKK1<sup>RNAi</sup>), 1587R-1 (*Crk*<sup>RNAi</sup>), 6313R-2 (*mask*<sup>RNAi#2</sup>), and 8222R-3 (*Pvr*<sup>RNAi#2</sup>).

Other transgenic lines from Bloomington Stock Center: #9490, *w*<sup>\*</sup>; TM6B, P{w[+mC]=*tubP-GAL80*}OV3, *Tb1*<sup>1</sup>/TM3, *Sb1* (Balancer Stock containing Gal80). #8529, *w*<sup>\*</sup>; P{w[+mC]=UAS-lacZ.Exel}2 (used as UAS control). #64196, *w*<sup>\*</sup>; P{UAS-Ras85D.V12}2 (constitutively active form of Ras85D) (Lee et al. 1996). #19989, P{y[+t7.7]=*Mae-UAS.6.11*}lic{GG01785}/FM7c (overexpresses MKK3) (Beinert et al. 2004). #59005, P{UAS-*p38b.DN*}1 (dominant negative form of *p38b*) (Adachi-Yamada et al. 1999). #5788, P{UAS-Ras85D.K}5-1 (wild type Ras85D) (Karim and Rubin 1998). #4845, P{UAS-Ras85D.N17}TL1 (dominant negative form of Ras85D) (Lee et al. 1996). #30139, *w*[1118]; P{w[+mC]=*Hml-GAL4.Delta*}2 (*hmlΔ-Gal4*). #30140, *w*[1118]; P{w[+mC]=*Hml-GAL4.Delta*}2, P{w[+mC]=UAS-2xEGFP}AH2 (*hmlΔ-Gal4*, UAS-GFP) (Sinenko and Mathey-Prevot 2004). #35544, *y*[1] *w*[\*]; P{y[+t\*] *w*[+mC]=UAS-Lifect-GFP}VIE-260B (UAS-lifect-GFP) (Hatan et al. 2011). #35837, *w*[1118]; P{Bac{y[+mDint2] *w*[+mC]=UAS-CD4-TdTom}VK00033 (UAS-CD4-TdTom) (Han et al. 2011).

### Scanning electron microscopy

Dissected larval epidermis (either unwounded or 4 h post pinch wounding) were fixed in 3% glutaraldehyde/2% paraformaldehyde with 2.5% DMSO in 0.2 M sodium phosphate buffer for 15 min. Samples were then dehydrated in graded ethanol concentrations and hexamethyldisilazane. Next, processed samples were mounted onto double-stick carbon tabs (Ted Pella, Inc., Redding, CA), which had been previously mounted onto glass microscope slides. The samples were then coated under vacuum using a Balzer MED 010 evaporator (Technotrade International, Manchester, NH) with platinum alloy for a thickness of 25 nm, then immediately flash carboncoated under vacuum. The samples were transferred to a desiccator for examination at a later date. Samples were examined/imaged in a JSM-5910 scanning electron microscope (JEOL, USA, Inc., Peabody, MA) at an accelerating voltage of 5 kV. To quantify the scanning electron microscopy (SEM) results, 3–5 (350×) images of each wound and 3–12 animals for each genotype were collected. These images were given to four or more persons to blindly score the hemocyte spreading phenotype. Percentages of hemocytes at the wound sites showing spreading morphology were binned into 0%, 25%, 50%, 75%, and 100%. Scoring results of each image from different persons were averaged. Multiple images from the same animals were then averaged to obtain a “spreading index.”

## Pvf1 enrichment

The plasmid containing Pvf1d (truncated version of Pvf1 containing only the VEGF-like domain) was transformed into BL21DE3 *E. coli* cells for overexpression. Cells were grown in Luria-Bertani broth at 37 °C to an  $A_{600}$  density of 0.6 and Pvf1d overexpression was achieved by induction with 1 mM isopropyl  $\beta$ -D-thiogalactoside (IPTG) for 3 h. Cell pellets were harvested and resuspended in lysis buffer containing 20 mM Tris pH8.0, 0.1 M NaCl, 5% glycerol, 1 mM ethylene diamine tetra-acetic acid, and 0.1 M dithiothreitol. Cells were lysed using a French press and the inclusion bodies containing the overexpressed Pvf1d were collected by centrifugation at 15,000 rpm for 30 min. Inclusion bodies were washed with the lysis buffer and stored in aliquots at  $-80^{\circ}\text{C}$ . Approximately 1 g of inclusion body was resuspended in lysis buffer containing 8 M urea and dialyzed overnight against the same buffer. Refolding of Pvf1d was achieved by overnight dialysis against buffer containing 50 mM N-cyclohexyl-3-aminopropanesulfonic acid (CAPS), pH 10.5, 50 mM NaCl, 5% glycerol, and 5 mM cysteine. Prior to dialysis, protein concentration was adjusted to 0.2 mg/ml and the dialysis step was repeated two more times. Subsequently, protein was cleared of precipitates by centrifugation and purified into a storage buffer containing 20 mM CAPS pH 10.5, 50 mM NaCl and 2.5% glycerol by size exclusion chromatography.

## In vitro hemocyte spreading assay

Hemocytes were isolated from wandering third instar larvae (genotype: *w; hml $\Delta$ -Gal4, UAS-GFP +/- UAS-RNAi transgene*) using a protocol modified from (Kadandale et al. 2010). Approximately 150 mg of larvae (~100) were collected into a cell strainer (70  $\mu\text{m}$  pore size) and washed once in phosphate-buffered saline (PBS). The rinsed larvae were crushed within the cell strainer in a 35 mm sterile cell culture dish with the cap-end of an eppendorf tube. The crushate containing hemocytes was filtered into the 35 mm dish by washing the crushed larvae twice with 500  $\mu\text{l}$  of PBS. The hemocyte-containing filtrate was collected into a 1.5-ml eppendorf tube and was centrifuged for 1 min at 1000 rpm to remove particulates. The supernatant was recentrifuged at 2000 rpm for 2 min to collect hemocytes. The hemocyte-containing pellet was resuspended in 500  $\mu\text{l}$  of room temperature Schneider's *Drosophila* culture medium (GIBCO, Invitrogen).  $\sim 1 \times 10^5$  cells suspended in the culture media described above were plated onto coverslips (Corning) that were placed in a sterile 24-well culture well (Corning). After plating, 1  $\mu\text{l}$  of 44 ng/ $\mu\text{l}$  recombinant Pvf1 protein was added to the culture and the cells were treated for 1 h at 25°C. One microliter of 1 $\times$  PBS was added to control cells instead of Pvf1 and were cultured for 1 h at 25°C. Phalloidin staining: after 1 h of Pvf1 or control treatment, the cells were washed once with PBS and fixed for 10 min with 4% paraformaldehyde before washing three times with PBS. The cells were permeabilized with 0.1% Triton X-100 (TX-100) in PBS (washing buffer) for 10 min and then incubated in blocking buffer (3% BSA, 0.1% TX-100 prepared in 1 $\times$  PBS) for 30 min at room temperature. The cells were stained overnight at 4°C with a 1:50 dilution of phalloidin-Alexa 546 (Invitrogen) made in blocking buffer followed by three washes each of 5 min. After washing, the coverslips containing phalloidin-stained cells were lifted off the well and mounted on to a glass slide (Fisher Scientific) using a drop (around 3  $\mu\text{l}$ ) of mounting media (Vectashield, Vector Laboratories). The coverslips were sealed to the glass slide with clear nail polish and stored at 4°C until imaged. Anti-Phospho-Pvr antibody staining: Phospho-Pvr (pPvr) antibody (monoclonal antibody) that detects the phosphorylation of Pvr at Tyr 1426

(Janssens et al. 2010) was a generous gift from Dr P. Rørth (Institute of Molecular and Cell Biology, Proteos, Singapore). Hemocytes were isolated and processed as mentioned above until the completion of blocking. Staining was performed with a 1:5 dilution of anti-pPvr (diluted in blocking buffer) at 4°C overnight. The secondary antibody was Goat anti-mouse DyLight 649 (Jackson ImmunoResearch Laboratories), which was bound for 1 h at room temperature before washing and mounting onto glass slides as described above.

## Hemocyte spreading screen

A more streamlined version of the above spreading assay was developed for the purposes of screening. In this protocol, select UAS-RNAi lines were crossed with the screening stock (*hml $\Delta$ -Gal4, UAS-lifect-GFP, UAS- $\lambda$ Pvr*) at 25°C. For each cross,  $\sim 10$  mid-3<sup>rd</sup> instar larvae (5 days after egg lay) carrying the Gal4 driver, UAS-lifect-GFP, UAS- $\lambda$ Pvr (UAS-Pvr<sup>CA</sup>) and the candidate UAS-RNAi transgene were selected and placed in a glass dissection well containing PBS. Larvae were washed with 70% ethanol and PBS and then briefly kept in 300  $\mu\text{l}$  of PBS. Hemocytes were released from the larvae by nicking their posterior ends with dissection scissors (Fine Science Tools, #15000-02). Collected hemocytes were transferred to an ice-cold low-retention tube (Fisher, #02-681-331). Collected hemocytes were seeded into an 8-well chamber slide (Millipore, PEZGS0816) and allowed to spread for 1 h at room temperature. After spreading, samples were fixed with 3.7% formaldehyde for 5 min, washed with PBS, and mounted in Vectashield before imaging with Olympus FV1000 Confocal microscope with Fluoview software and 60 $\times$  oil lens. ImageJ was used to manually measure the longest axis of individual hemocytes. Overlapping hemocytes were excluded from measurement to avoid potential interference between cells. To measure the hemocyte size before spreading, hemocytes were fixed (as above) right after isolation and washed with PBS before resuspending in Vectashield and mounting onto slides for imaging.

## Lethality suppressor screen

Candidate UAS-RNAi lines were crossed with the screening stock (UAS-Pvr; A58-Gal4/TM6B, tubP-Gal80) at 22.5°C, at which the best signal to noise ratio of the screen was observed. Flies were transferred onto fresh vials every 2 days. UAS-Luciferase<sup>RNAi</sup> and UAS-Pvr<sup>RNAi#2</sup> were used as negative and positive controls, respectively. Larvae, pupae, and/or adults emerging from the different crosses were observed 6–9 days after egg laying. The UAS-Luciferase<sup>RNAi</sup> control group does not survive to the prepupal and pupal stages, whereas the UAS-Pvr<sup>RNAi#2</sup> group survives until adult stage. Candidate genes were scored as putative suppressors when their corresponding UAS-RNAi transgenes delayed the lethal stage to prepupae or pupae. Median suppression was defined by the observation of three to five pupae/prepupae in a single vial (annotated in Figure 3C with "+"). Strong suppression was defined by the observation of six or more pupae/prepupae in a single vial (annotated in Figure 3C with "++"). No suppression "-" or variable suppression across multiple trials "+/-" were annotated in Figure 3C.

## Larval wound closure assay

Pinch wounding of the larvae was carried out according to our detailed protocol (Burra et al. 2013). In cases where early expression of a UAS transgene was lethal (UAS-Akt<sup>RNAi</sup>), larvae bearing *tub-gal80<sup>5</sup>*, the Gal4 driver and toxic UAS transgene were raised for 6 days at 18 °C to begin development, shifted to 32 °C for 2 days to reach mid-third-instar, and then allowed to recover at 25 °C

following pinch wounding. Pinch wounds were scored as “open” if the initial wound gap remained after 24 h, and as “closed” if a continuous epidermal sheet was observed at the wound site. To calculate the percentage of larvae with open wounds, three sets of  $N \geq 8$  per genotype were pinched and scored for open wounds under a fluorescent stereo microscope (Leica MZ16FA with Planapo 1.6× objective and appropriate filters). To further examine wound morphology, the third instar larval epidermis was dissected and processed as detailed previously (Burra et al. 2013). To highlight epidermal morphology, a mouse monoclonal antibody against Fasciclin III was used (1:50; Developmental Studies Hybridoma Bank). An Olympus FV1000 Confocal microscope, Olympus 20× oil lens and Fluoview software were used to obtain images of the dissected epidermal whole mounts.

### Wholemout immunofluorescence

Larval epidermal wholemounts were dissected and fixed with 3.7% formaldehyde at 4°C overnight followed by blocking in PBS with 1% heat inactivated goat serum and 0.3% triton X-100 for 1 h at room temperature. Samples were then incubated with the following primary antibodies overnight at 4°C: Mouse anti-Fasciclin III (1:50; Developmental Studies Hybridoma Bank) was used to label epidermal cell boundaries and Rabbit anti-activated caspase 3 (BD Biosciences, cat # 559565, 1:200) was used to detect apoptotic cells. After washing with 0.3% triton X-100 in PBS (PBST), tissues were incubated with goat anti-mouse Alexa 488 antibodies (Invitrogen A11001, 1:500) and goat anti-rabbit Alexa 647 (life technologies, A21244, 1:500) for 3 h at room temperature before washing with PBST, mounting (VECTASHIELD, Vector laboratories, H1000-10) and imaging using an Olympus FV1000 as described above.

### Statistical analyses

For statistical analysis of the WC phenotype between genotypes, one-way ANOVA (Dunn’s multiple comparisons) were used to test the significance of experiments.

For statistical analysis of hemocyte spreading, if the data of all the genotypes passed D’Agostino and Pearson omnibus normality test, unpaired two-tailed t-test (two groups) or one-way ANOVA (more than two groups, Dunn’s multiple comparisons) were used to test the significance of experiments. When data from one or more genotypes did not pass D’Agostino and Pearson omnibus normality test, Kolmogorov–Smirnov test (two groups) or Kruskal–Wallis test (more than two groups, Dunn’s multiple comparisons) were used to test the significance of experiments. For all quantitations: ns, not significant; \* $P < 0.05$ ; \*\* $P < 0.01$ ; \*\*\* $P < 0.001$ ; \*\*\*\* $P < 0.0001$ .

## Results

### Pvr and Pvf1 are required for hemocyte spreading at wound sites

In *Drosophila* larvae, circulating hemocytes adhere to wound sites if they encounter the wound surface by chance (Babcock et al. 2008). Once there, they assume a spread morphology and phagocytose wound-associated debris (Babcock et al. 2008). We sought to identify factors that might be responsible for hemocyte spreading *in vivo*. We began our search with transmembrane proteins known to be expressed on hemocytes and known to affect hemocyte biology. Pvr (platelet-derived growth factor/VEGF-related receptor) fits these criteria (Heino et al. 2001; Cho et al. 2002; Bruckner et al. 2004). To observe hemocytes at wound sites, we pinch-wounded (Burra et al. 2013) third instar *Drosophila* larvae

and used scanning electron microscopy (SEM) to examine the morphology of wound-adherent hemocytes (see schematic in Figure 1A). In control larvae (Figure 1B, see also Supplementary Table S1 for list of genotypes relevant to each figure panel) large numbers of hemocytes bound to the wound and assumed a spread morphology. In *Pvr<sup>null/hypo</sup>* (see Materials and methods and Supplementary Table S1 for allele designations) there were much fewer hemocytes at the wound site (Figure 1C). This is to be expected, as Pvr is required for hemocyte survival in embryos (Bruckner et al. 2004). Further, Pvr activation (Zettervall et al. 2004) or Pvf2 overexpression (Munier et al. 2002) can drive hemocyte proliferation at the larval stage. We also observed greatly reduced hemocyte numbers in *Pvf2<sup>hypo</sup>* and in *Pvf3<sup>null</sup>* mutants at the wound sites (Figure 1, D and E), suggesting that these ligands may also be required for hemocyte survival. The third VEGF-like ligand, Pvf1, showed a different phenotype at wound sites (Figure 1F) compared to *Pvf2* and *Pvf3* mutants. While hemocytes were present in substantial numbers at wound sites within *Pvf1<sup>null</sup>* larvae, closer examination revealed that they possessed a morphology distinct from controls. Higher magnification views of control larvae (Figure 1G) show that spread hemocytes formed a dense and interlinked network of cell processes over the wound site. In *Pvf1<sup>null</sup>* mutants the hemocytes adhered, but had a distinctly rounded morphology, with few broad and flattened membrane sheets, even when in close proximity to each other (Figure 1H). Quantitation of the spreading index (see Materials and methods and Supplementary Figure S1 which illustrates the scoring metric used) between these two genotypes revealed a significant difference in visible morphology (Figure 1I). In sum, Pvr and two of its ligands, Pvf2 and Pvf3, are required for normal numbers of wound-adherent hemocytes, while Pvf1 is required for these cells to assume a spread morphology at the wound site.

### In vitro assays for hemocyte spreading: a flattened lamellar morphology induced by Pvf1 application or Pvr activation

*In vivo* loss of function analysis suggested that Pvf1, possibly through the Pvr receptor, is required for hemocyte spreading. We tested this in another way, by modifying an *in vitro* assay for hemocyte spreading (Figure 2A) (Kiger et al. 2003; D’Ambrosio and Vale 2010). Lineage-labeled plasmatocytes (*hmlΔ-Gal4, UAS-GFP*) were collected from third instar larvae, plated, and exposed to enriched (Supplementary Figure S2A) Pvf1 VEGF-like domain (see Materials and methods). This enriched protein was active, as assessed by its ability to cause Pvr phosphorylation in isolated hemocytes (Supplementary Figure S2, B and B’). The phosphorylation signal was specific, as it depended upon Pvr expression in the isolated hemocytes (Supplementary Figure S2, C and C’).

Control hemocytes plated *in vitro* assumed a rounded morphology, as assessed by the cytoplasmic GFP label (Figure 2B). When stained with phalloidin, which labels filamentous actin, these cells exhibited a peripheral ring of dense actin filaments (Figure 2B, top row). Exposure to enriched and active Pvf1 VEGF-like domain during the period of plating altered the morphology of these cells—they now exhibited a large lamellipodial-like fan extending outwards from the peripheral actin ring (Figure 2B, bottom row). To determine whether this *in vitro* Pvf1-dependent spreading requires the Pvr receptor, we isolated hemocytes coexpressing a *UAS-Pvr<sup>RNAi</sup>* transgene whose efficacy has been verified in other assays (Wu et al. 2009; Lopez-Bellido et al. 2019). In the absence of exogenous Pvf1 protein, hemocytes expressing *UAS-Pvr<sup>RNAi#2</sup>* had a morphology and actin distribution similar to controls (Figure 2C, top row). These same cells, when plated in the

## Hemocytes at the wound (Scanning Electron Microscopy)

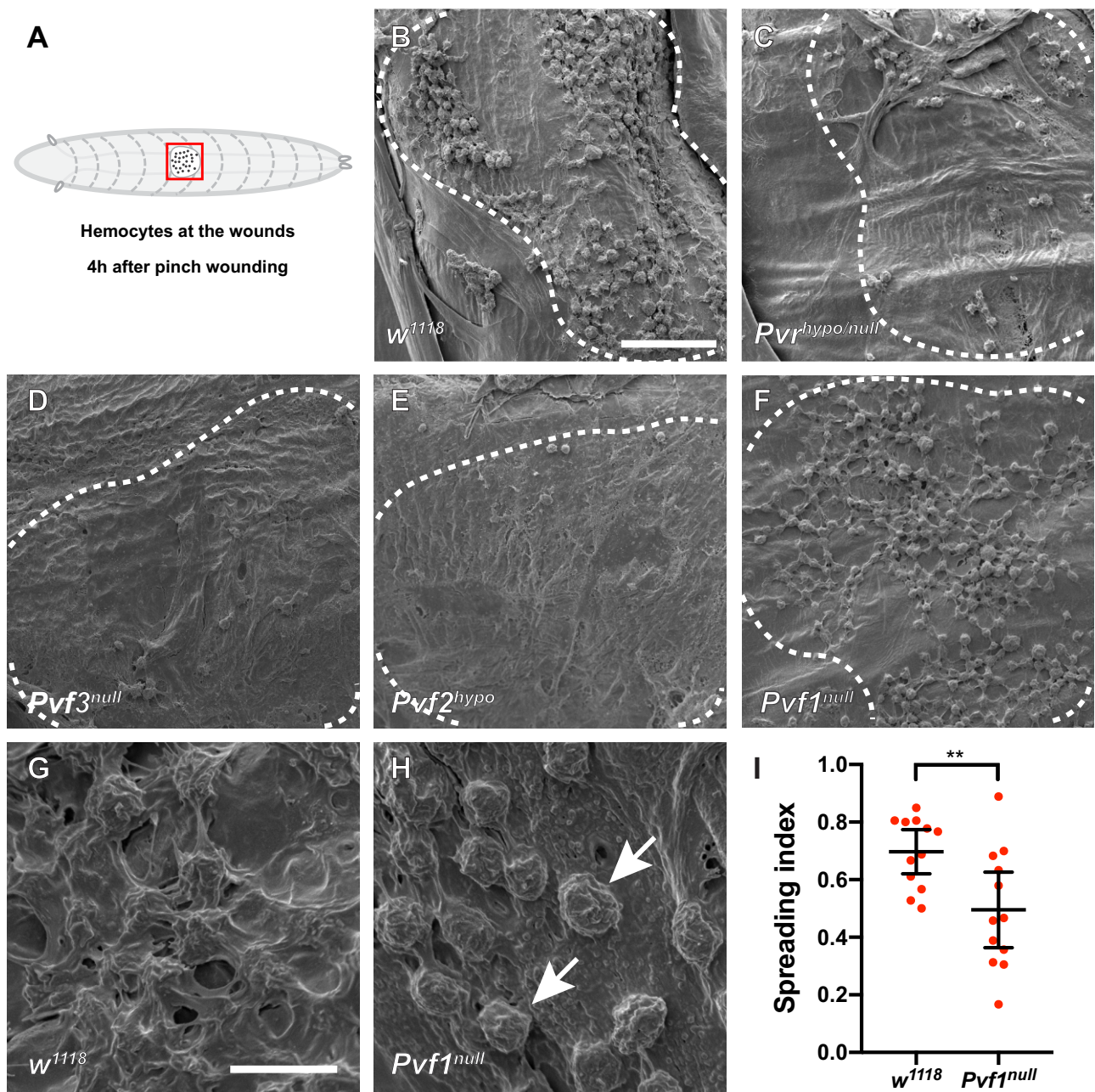


**Figure 1** Pvr and Pvf1 are required for hemocyte spreading at larval wound sites. (A) Cartoon of third instar *Drosophila* larva (anterior to left, posterior to right) red square highlighting the region of interest (clear oval, the wound, and black dots, hemocytes) for scanning electron microscopy (SEM) analysis of pinch wounds. (B–H) Scanning electron micrographs of wounded and dissected third instar larvae of the indicated genotypes to visualize wound-adherent blood cells. Dashed white lines—outlines of pinch wound sites. (B) *w<sup>1118</sup>* control, (C) *Pv<sup>null/hypo</sup>*, (D) *Pvf3<sup>null</sup>*, (E) *Pvf2<sup>hypo</sup>*, (F) *Pvf1<sup>null</sup>*. Scale bar in (B) = 50  $\mu$ m and applies to (B–F). (G) Close-up of spread hemocytes, *w<sup>1118</sup>*. (H) Close-up of unspread hemocytes indicated by arrows, *Pvf1<sup>null</sup>*. Scale bar in (G) = 10  $\mu$ m and applies to (G and H). (I) Quantitation of blood cell spreading in control larvae vs *Pvf1<sup>null</sup>* mutant larvae.  $n = 12$ . Data are mean with 95% CI. \*\* $P < 0.01$  (unpaired two-tailed t-test).

presence of Pvf1 protein, exhibited an apparent increase in cellular actin staining but did not spread outwards to form a lamellipodial fan (Figure 2C, bottom row).

Finally, we determined whether hyperactivation of Pvr *in vivo* through expression of the constitutively active UAS-*Pvr<sup>CA</sup>* transgene (Duchek et al. 2001) could directly lead to spreading of hemocytes. Hemocytes expressing a UAS-*LifeactGFP* transgene (to label filamentous actin) and a UAS-*control<sup>RNAi</sup>* transgene

(Figure 2D) possessed a simple rounded morphology *in vitro*. By contrast, hemocytes coexpressing UAS-*Pvr<sup>CA</sup>* and UAS-*Luciferase<sup>RNAi</sup>* transgene (to equalize the number of UAS transgenes in the experimental setup) exhibited prominent lamellipodial fans (Figure 2E) similar to those observed upon coculture with the Pvf1 VEGF-like domain (Figure 2B, bottom row). The spreading phenotype of different genotypes was measured based on the average of individual cell diameters measured at the

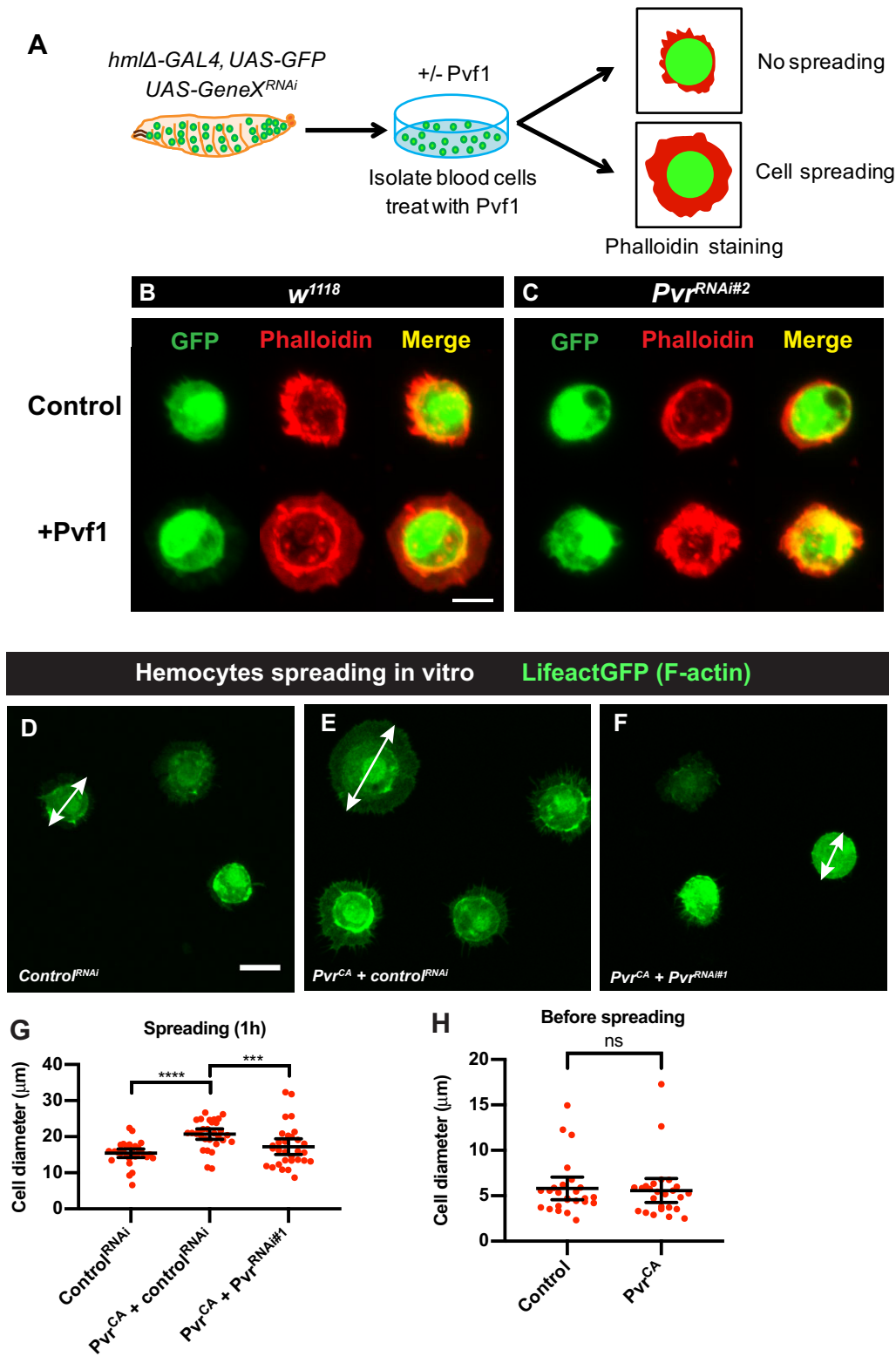


**Figure 2** Testing the role of Pvr/Pvf1 in hemocyte spreading with in vitro assays. (A) Schematic of hemocyte spreading assay for treatment with Pvf1. (B) Untreated control hemocytes (*w<sup>1118</sup>; hmlΔ-Gal4, UAS-GFP*) and treated (+ enriched Pvf1 protein) hemocytes are shown. Blood cells were harvested from larvae, plated in vitro, fixed, and visualized with the GFP lineage label (green, left column), phalloidin to label filamentous actin (red, middle column), or both (merge, right column) in the absence (top row) or presence (bottom row) of enriched Pvf1 protein. Scale bar in (B) = 10 μm and applies to (B and C). (C) Same experiment as in (B) but now the hemocytes are also expressing a *UAS-Pvr<sup>RNAi</sup>* transgene (bottom row) or not (top row) to test whether the spreading response observed upon addition of Pvf1 protein depends on functional Pvr expression. (D–F) Morphology of plated hemocytes (*w<sup>1118</sup>; hmlΔ-Gal4, UAS-LifeActGFP*, green) with the indicated transgenes. Scale bar in (D) = 10 μm and applies to (D–F). Double-headed arrows are examples of the longest cell diameters. (D) *UAS-Control<sup>RNAi</sup>*. (E) *UAS-Pvr<sup>CA</sup> + UAS-Control<sup>RNAi</sup>*. (F) *UAS-Pvr<sup>CA</sup> + UAS-Pvr<sup>RNAi#1</sup>*. (G and H) Quantitation of hemocyte cell diameters (μm) of the indicated genotypes after 1 h of plating (G) or before plating (H) to test whether expression of *UAS-Pvr<sup>CA</sup>* affects hemocyte size in any way. (G, H) Each dot represents the longest diameter of a single cell. Error bars: mean with 95% CI. (G) *n* = 30 (Kruskal–Wallis multiple comparisons test). (H) *n* = 25; ns, not significant (Kolmogorov–Smirnov test).

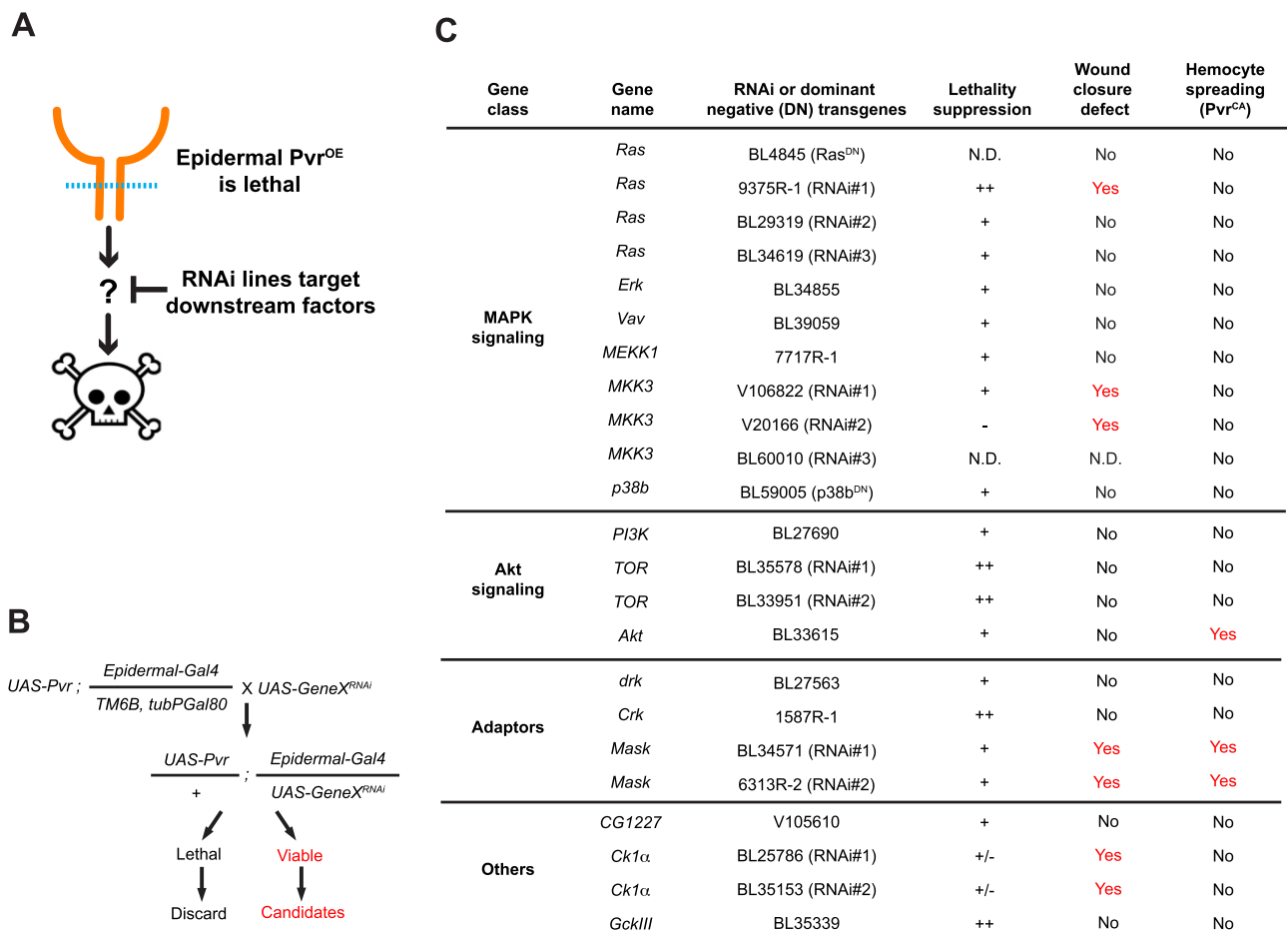


**Figure 3** Targeted genetic screen for suppressors of Pvr-induced lethality. (A) Conceptual schematic of genetic screen. Pvr overexpression in the larval epidermis is lethal. We screened for RNAi lines (targeting possible/probable downstream components of RTK signaling) that, when coexpressed with Pvr, could suppress this lethality. (B) Genetic scheme of the screen, illustrating the genotypes, crosses, and scoring involved. (C) Lethality suppressors from the screen, organized by gene class. Also shown are whether the suppressors affected epidermal WC at the larval stage and/or hemocyte spreading in the *in vitro* assay (see Figure 2). For the strength of lethality suppressions: ++, strong suppression. +, median suppression. -, no suppression. +/-, variable suppression effects. N.D., not determined.

longest axis for each cell. Cell diameters of hemocytes expressing UAS-Pvr<sup>CA</sup> and UAS-control<sup>RNAi</sup> were significantly larger than control (Figure 2G). The presence of UAS-Pvr<sup>CA</sup>-induced lamellipodial fans was dependent upon Pvr, as coexpression of UAS-Pvr<sup>CA</sup> and UAS-Pvr<sup>RNAi#1</sup> led to hemocytes with a simple rounded morphology (Figure 2, F and G). The fan-like morphology of hemocytes expressing activated Pvr was not simply due to an increase in the original size of the hemocytes. When we measured cell size before plating (Figure 2H, see representative micrographs in Supplementary Figure S3), there was no difference in the cell diameter of hemocytes expressing UAS-Pvr<sup>CA</sup> vs controls. By contrast, UAS-Pvr<sup>CA</sup>-expressing hemocytes were of significantly greater diameter 1 h after plating, an effect that was dependent upon expression of Pvr (Figure 2G). Together, these data demonstrate that Pvf1 causes hemocyte spreading via Pvr activation.

### A suppressor screen for genes that act downstream of Pvr signaling

Pvr signaling has a unique place in *Drosophila* tissue damage responses in that it is required in multiple tissues for diverse cellular responses. In the larval epithelium, Pvr is required for WC (Wu et al. 2009), in nociceptive sensory neurons for the perception of noxious mechanical stimuli (Lopez-Bellido et al. 2019), and in

hemocytes for spreading at wound sites (Figure 1). A challenge in studying this pathway has been that there are no broadly useful reporters of downstream pathway activity. The anti-phospho-Pvr antibody used in Supplementary Figure S2 is only useful on isolated cells and not for wholemount tissue stains (data not shown). Given these challenges, we designed a genetic screen to efficiently identify genes that act downstream of Pvr activation. To do this, we took advantage of the fact that overexpression of Pvr in the *Drosophila* larval epidermis is lethal (Wu et al. 2009). The screen itself is a lethality suppressor screen (see conceptual schematic in Figure 3A). We reasoned that coexpression of UAS-RNAi transgenes targeting potential downstream genes would suppress the lethality induced by overexpression of Pvr. The screening stock(s) and crossing scheme for the screen is depicted in Figure 3B and hinges on the use of the Gal80 system (Vef et al. 2006) to suppress expression of UAS-Pvr and keep the screening stock alive. The candidate set of UAS-RNAi lines included known kinases and adaptors that act downstream of RTKs as well as a broader set of such genes (see Supplementary Table S2). The first phenotype screened was the presence of pupae in the vials coexpressing UAS-Pvr and the UAS-GeneX<sup>RNAi</sup> transgenes. In total, 530 genes were screened and 15 lethality suppressors were obtained (Figure 3C). Many of the basic components of mitogen-activated

protein kinase and Akt signaling, as well as a subset of common RTK adaptors and other kinases scored positive as suppressors. Ultimately, all of the lethality suppressors (and further RNAi or dominant-negative transgenes targeting them) were also screened for phenotypes in larval WC and *in vitro* hemocyte spreading (Figure 3C, right columns) and a subset of these phenotypes are shown in the ensuing figures.

### New wound closure genes: Ras, MKK3, and Mask

In the ideal case, Pvr signaling architecture would be similar between Pvr-induced lethality and WC and most or all of the lethality suppressors would then score positive as genes required for larval WC. This was not in fact observed (see Discussion section for possible explanations). Only a specific subset of the lethality suppressors were also identified as WC genes. When *UAS-Luciferase<sup>RNAi</sup>* transgenes (negative control) are expressed in the larval epidermis, pinch wounds close (Figure 4A). By contrast, when *UAS-Pvr<sup>RNAi</sup>* transgenes are expressed (Figure 4B, positive control) pinch wounds remain open at 24 h post-wounding. The open-wound phenotypes observed upon expression of *UAS-RNAi* transgenes targeting Ras, a small GTPase (Figure 4C), Mask, an adaptor protein (Figure 4D), and MKK3, an MAP kinase kinase (Figure 4E) are shown in Figure 4, as is quantitation of the prevalence of these phenotypes (Figure 4F). The lethality suppressor screen, while not perfect, was nonetheless quite fruitful at expanding our collection of known WC genes beyond the JNK and actin pathways (Lesch et al. 2010; Brock et al. 2012). Other genes that scored positive in this screen (CK1 $\alpha$ ) were also found in an analysis of adherens junctions at larval wound sites (Tsai and Galko 2019).

Which, if any, of the identified WC genes act downstream of Pvr in the context of larval WC? We designed an experimental strategy (coexpression of *UAS-Pvr<sup>RNAi</sup>* and a *UAS-cDNA* transgene for candidate genes) that would test this possibility. Certainly, suppression of the full WC defect caused by *UAS-Pvr<sup>RNAi</sup>* is a high bar, and might only be expected to be observed for those genes at or close to the top of the signaling pathway. Coexpression of an irrelevant gene (*UAS-LacZ*, negative control) was not capable of suppressing the open-wound phenotype observed upon expression of *UAS-Pvr<sup>RNAi</sup>* (Figure 4G) indicating that titrating the Gal4/*UAS* system with an additional *UAS* sequences, by itself, was insufficient to suppress the WC phenotype. By contrast, coexpression of *UAS-Pvr* (positive control) suppressed the open-wound phenotype of *UAS-Pvr<sup>RNAi</sup>* (Figure 4H) about half of the time (Figure 4K). Ras suppressed at a similar level (Figure 4, I and K) while MKK3 (Figure 4, J and K) was slightly weaker. Ck1 $\alpha$  and Mask could not suppress (Figure 4K). Of note, none of the *UAS-cDNA* overexpression transgenes caused an open wound phenotype on their own (Figure 4K, right side). In sum, we have identified a number of new larval WC genes, some of which, by genetic epistasis, can be placed downstream of Pvr in this particular process.

### Mask and Akt act downstream of Pvr to mediate hemocyte spreading *in vitro*

We devised a parallel strategy to determine which of the Pvr lethality suppressors act downstream of Pvr in hemocyte spreading. This analysis was somewhat simpler, as we could ask whether each lethality suppressor could also suppress the hemocyte spreading induced by hemocyte expression of *UAS-Pvr<sup>CA</sup>* (see Figure 5A, schematic and Figure 5B, control). Coexpression of *UAS-RNAi* transgenes targeting either Akt (Figure 5, C and E) or Mask (Figure 5, D and F) resulted in a decrease of the expanded

hemocyte cell diameter typically seen upon expression of *UAS-Pvr<sup>CA</sup>*. By contrast, *UAS-RNAi* and/or *UAS-DN* transgenes targeting MKK3 (Figure 5G), Ck1 $\alpha$  (Figure 5H), or Ras (Figure 5I) did not block *Pvr<sup>CA</sup>*-induced hemocyte spreading. Importantly, expressions of either *UAS-Akt<sup>RNAi</sup>* or *UAS-Mask<sup>RNAi</sup>* did not affect basal hemocyte spreading after 1 h as measured by cell diameters (Figure 5J). While some of the genes analyzed (in particular Ras, Ck1 $\alpha$ , and MKK3) caused a general/baseline decrease in basal hemocyte spreading (Figure 5J), *Pvr*-induced spreading was compared to the relevant baseline for each gene (Figure 5, E–I). These results demonstrate that some Pvr downstream factors (Mask) are shared between larval epidermal WC and hemocyte spreading while others, (Akt, Ck1 $\alpha$ , MKK3, Ras) are specific for a particular cellular response.

### Mask is also required for hemocyte spreading at wound sites *in vivo*

We next analyzed, using the SEM assay introduced in Figure 1, whether genes that have phenotypes in the *in vitro* hemocyte spreading assay (Mask and Akt) also affected wound-induced hemocyte spreading *in vivo*. As observed previously, control hemocytes typically form a dense lawn on the wound surface (Figure 6A) and, when analyzed at higher magnification, exhibit fan-like lamellipodial extensions either toward each other or toward the cuticle surface (Figure 6D). In larvae expressing *UAS-Mask<sup>RNAi</sup>* in hemocytes, the wound-adherent cells appeared less dense (Figure 6B) and possessed a wrinkled but rounded morphology that did not include lamellipodia extending either toward each other or the cuticular surface (Figure 6E). Visualization of apoptosis in wound-adherent hemocytes using an antibody against activated Caspase-3 revealed that there was no substantial colocalization of apoptotic cells and wound-adherent hemocytes in wounded larvae expressing *UAS-Mask<sup>RNAi</sup>* or in *Puf1<sup>null</sup>* larvae compared to UV-irradiated larvae which contained apoptotic epidermal cells as a positive control (Supplementary Figure S4). In larvae expressing *UAS-Akt<sup>RNAi</sup>* in hemocytes (Figure 6C), there appeared to be a survival defect similar to that observed for the Pvr, Pvf2, and Pvf3 ligands (Figure 1, C–E), as very few hemocytes were observed at the wound site. Quantitation of the spreading index in control vs *UAS-Mask<sup>RNAi</sup>*-expressing hemocytes (Figure 6F) revealed a significant defect in spreading, indicating that for this gene, the *in vitro* spreading defect was an accurate predictor of a requirement for spreading *in vivo*.

## Discussion

In this study, we establish a new role for Pvf1/Pvr signaling in regulating wound-induced blood cell spreading at the larval stage. Several lines of evidence suggest that the Pvf1 ligand and its Pvr receptor are required for blood cell spreading. First, blood cells in Pvf1 mutants show a rounded morphology at wound sites, unlike the typical spread morphology in controls. Second, Pvf1 can directly induce blood cell spreading *in vitro* in a manner that depends upon function of Pvr. Finally, Pvr hyperactivation promotes hemocyte spreading in primary cultures of larval hemocytes. Together these loss- and gain-of-function experiments strongly suggest that Pvf1 and Pvr are required for blood cell spreading. In this study, we also developed a new screening platform to try to identify genes that might function downstream of Pvr in the various wound responses for which it is required. This genetic screen for suppression of Pvr-induced lethality identified a number of genes, some of which have strong phenotypes affecting WC, hemocyte spreading, or both. Below, we discuss the

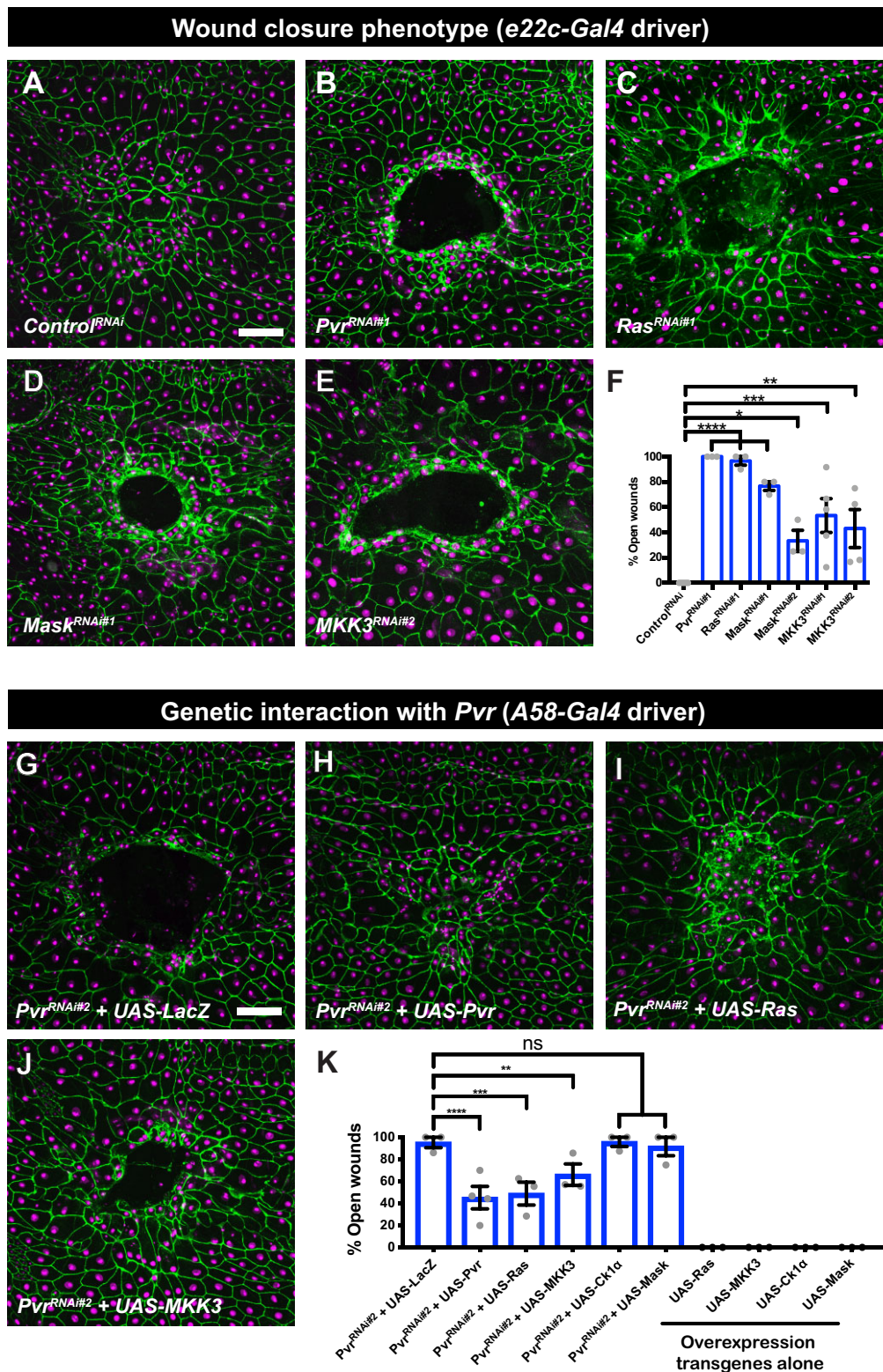


**Figure 4** Epidermal WC phenotypes of select suppressors of Pvr-induced lethality and genetic interactions with Pvr. (A–E) Dissected epidermal whole mounts of wounded third instar larval epidermis, expressing UAS-*dsRed2Nuc* (nuclei, magenta) and UAS-*src-GFP* (GFP, not shown) and expressing the indicated transgenes via *e22c-Gal4* driver, immunostained with anti-Fasciclin III (green). Open wounds appear as dark holes in the center. (A) UAS-Control<sup>RNAi</sup>, (B) UAS-Pvr<sup>RNAi#1</sup>, (C) UAS-Ras<sup>RNAi#1</sup>, (D) UAS-Mask<sup>RNAi#1</sup>, (E) UAS-MKK3<sup>RNAi#2</sup>. Scale bar, 50  $\mu$ m in (A) is for (A–E). (F) Quantitation of larval WC phenotypes (% open wounds) vs genotype. Each dot represents one set of  $n \geq 8$ . Total three or more sets for each genotype. Error bar, mean  $\pm$  SEM. One-way ANOVA with Dunn's multiple comparisons. \*\*\*\* $P < 0.0001$ , \*\*\* $P < 0.001$ , \*\* $P < 0.01$ , \* $P < 0.05$ . (G–J) Epistasis. Ability of overexpression of select WC genes to rescue the WC phenotype of UAS-Pvr<sup>RNAi#2</sup>. Genotype of all panels: *w<sup>1118</sup>; UAS-Pvr<sup>RNAi#2</sup>/+; A58-Gal4, UAS-*dsRed2Nuc*, UAS-*src-GFP* (not shown) plus the indicated overexpression transgene. (G) UAS-Pvr<sup>RNAi#2</sup> + UAS-*lacZ*. (H) UAS-Pvr<sup>RNAi#2</sup> + UAS-Pvr. (I) UAS-Pvr<sup>RNAi#2</sup> + UAS-Ras. (J) UAS-Pvr<sup>RNAi#2</sup> + UAS-MKK3. Scale bar, 50  $\mu$ m in (G) is for (G–J). (K) Quantitation of epistasis experiments—% Open wounds vs the indicated genotypes. Each dot represents one set of  $n \geq 8$ . Total three or more sets for each genotype. Error bar, mean  $\pm$  SEM. One-way ANOVA multiple comparisons. \*\*\*\* $P < 0.0001$ , \*\*\* $P < 0.001$ , \*\* $P < 0.01$ , ns, not significant.*

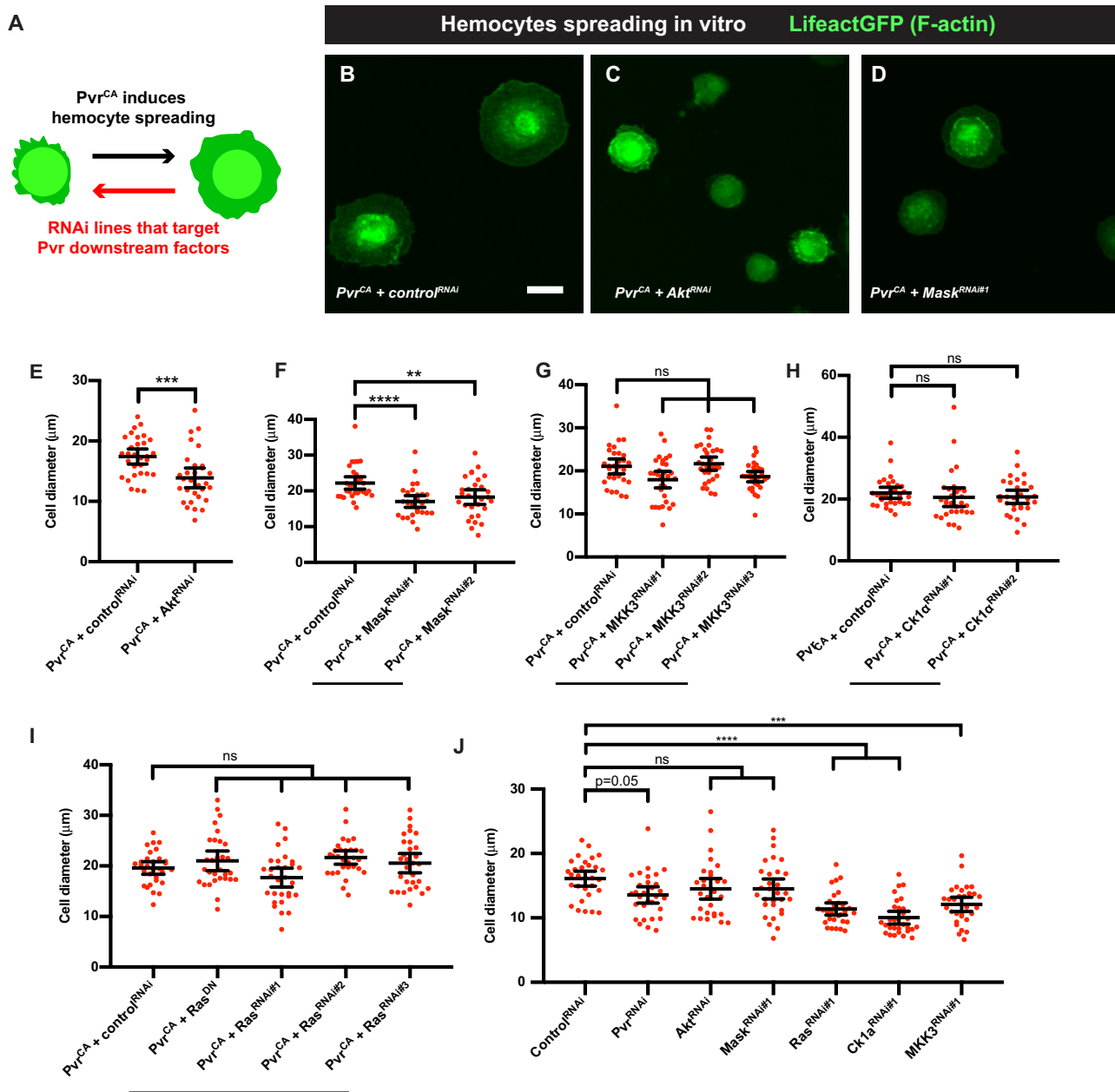


**Figure 5** Hemocyte spreading phenotypes of select suppressors of Pvr-induced lethality. (A) Conceptual schematic of hemocyte spreading assay. Overexpression of a constitutive active form of Pvr (Pvr<sup>CA</sup>) in the larval hemocytes promote cell spreading. We screened for lethality suppressor RNAi lines that, when coexpressed with Pvr<sup>CA</sup>, could suppress the spreading phenotype. (B–D) Hemocyte morphology of hemocytes harvested from larvae of the genotype (*UAS-Pvr<sup>CA</sup>, hmlΔ-Gal4, UAS-LifeactGFP*) plus the indicated transgenes, plated 1 h in vitro, and visualized by the actin/lineage label (green). (B) *UAS-Pvr<sup>CA</sup> + control<sup>RNAi</sup>*. (C) *UAS-Pvr<sup>CA</sup> + UAS-Akt<sup>RNAi</sup>*. (D) *UAS-Pvr<sup>CA</sup> + UAS-Mask<sup>RNAi#1</sup>*. (E–J) Quantitation of hemocyte diameter (spreading) vs the indicated genotypes targeting particular genes. Each dot represents a single cell. *n* = 30. Error bars: mean with 95% CI. \*\*\*\**P* < 0.0001. \*\*\**P* < 0.001. \*\**P* < 0.01. ns, not significant. (E) Akt. Unpaired t-test. (F) Mask. Kruskal–Wallis multiple comparisons test. (G) MKK3. Kruskal–Wallis multiple comparisons test. (H) Ck1α. Kruskal–Wallis multiple comparisons test. (I) Ras. One-way ANOVA multiple comparison. (J) Expressions of *UAS-Akt<sup>RNAi</sup>* and *UAS-Mask<sup>RNAi</sup>* in hemocytes did not affect basal spreading, while *UAS-Ras<sup>RNAi</sup>*, *UAS-Ck1α<sup>RNAi</sup>*, and *MKK3<sup>RNAi</sup>* reduced basal spreading. Kruskal–Wallis multiple comparisons test.

implications of these findings for wound-induced hemocyte responses, the diversity of Pvr signaling effects in different cell types, and the architecture of signaling downstream of Pvr in different wound-responsive cell types.

Larvae possess a population of circulating hemocytes that are distributed throughout the open body cavity and patrol for tissue damage (Brock et al. 2008). Hemocytes that happen to bump into the wound adhere and spread (Babcock et al. 2008). Our work here suggests that adhesion and spreading are separable phenomena

because in *Pvf1* mutants and in larvae expressing *UAS-Mask<sup>RNAi</sup>* in hemocytes, attachment to wound sites occurs normally though subsequent spreading at the wound surface does not. In both of these genotypes, the circulating hemocyte populations appear qualitatively normal. In the fly embryo, Pvr and several of its ligands are required for survival (Bruckner et al. 2004) and for developmentally programmed hemocyte migrations (Wood et al. 2006; Parsons and Foley 2013) but not for recruitment to wounds (Wood et al. 2006). Other signaling pathways such as TNF are

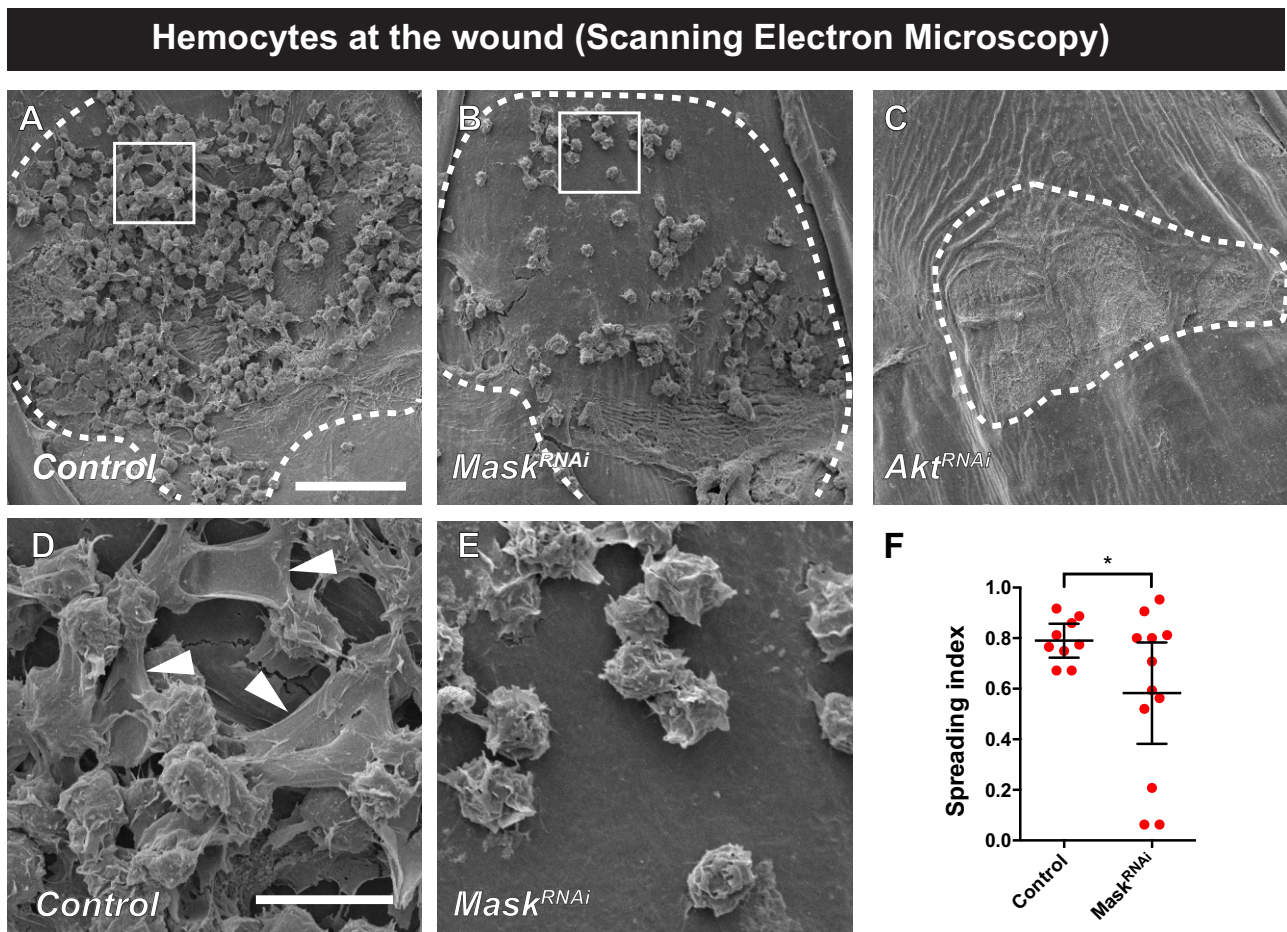


**Figure 6** Mask is required for hemocyte spreading at wound sites. (A–E) Scanning electron micrographs of wounded and dissected third instar larvae of the indicated genotypes to visualize wound-adherent blood cells. (A) Control. (B) *UAS-Mask<sup>RNAi</sup>*. (C) *UAS-Akt<sup>RNAi</sup>*. (D) Control—close-up image of white box in (A). Arrowheads indicate hemocyte lamellae. (E) *UAS-Mask<sup>RNAi</sup>*—close-up image of white box in (B). In all panels (A–E), the bare larval cuticle and cell debris is underneath the attached hemocytes [see outlined region in (C) which lacks attached hemocytes]. (F) Quantitation of hemocyte spreading index at wound sites in control and *UAS-Mask<sup>RNAi</sup>*-expressing larvae. Unpaired t-test.

required for an invasive-like transmigration near the embryo head (Ratheesh et al. 2018). The differential role of Pvr and its ligands in embryos and larvae highlight another dimension to the interesting stage-specific differences in hemocyte recruitment to damaged tissue (Brock et al. 2008; Ratheesh et al. 2015). There are other contexts besides wound-induced inflammation where hemocytes adhere to both normal and foreign cellular surfaces in *Drosophila*. These include sessile compartments (Bretscher et al. 2015), transformed tissue (Pastor-Pareja et al. 2008), and parasitic wasp eggs (Russo et al. 1996; Williams et al. 2005). It will be interesting to see in future studies if Pvf/Pvr signaling also plays a role in these events.

In addition to its roles in various developmental processes (McDonald et al. 2003; Ishimaru et al. 2004; Harris et al. 2007; Garlena et al. 2015), Pvf/Pvr signaling is required for a diverse array of tissue damage responses including epidermal WC (Wu et al. 2009), mechanical nociception (Lopez-Bellido et al. 2019), and larval hemocyte spreading during inflammation (this study). Both *in vitro* using S2 cells (Friedman and Perrimon 2006) and *in vivo* using glial cells (Kim et al. 2014) Pvr signaling screens have been carried out in other contexts. However, it has been a challenge to identify downstream Pvr signaling components that function in WC due to the lack of a pathway reporter that functions well *in vivo*. To circumvent this, we designed a genetic

suppressor screen that exploits the fact that overexpression of Pvr in the larval epidermis is lethal (Wu et al. 2009). The reasons for this lethality are not clear but could potentially be related to a general hyperactivation of the epidermal WC response. If this hypothesis was correct, it might be expected that most identified lethality suppressors would also be required for WC. This was not observed. While a substantial set of the lethality suppressors were not found to affect WC, three factors—Ras, Mask, and MKK3—did affect WC. This divergence between lethality suppressors and WC genes could indicate a role for Pvr in maintaining the integrity or survival of the larval epidermis. Indeed, some of the genes found here overlap with Pvr signaling components found to be important for hemocyte survival (Sopko et al. 2015).

The three suppressors of Pvr-induced lethality that were also found here to be required for WC include Ras, a small GTPase; MASK, an adaptor protein required for RTK signaling in other contexts (Smith et al. 2002); and MKK3, a Map kinase (Han et al. 1998). Epistasis analysis (overexpression of putative downstream Pvr genes in a Pvr-deficient background) revealed that only those components very close to Pvr in the presumed signaling cascade (Pvr itself and the Ras GTPase) were capable of partially rescuing the WC defect resulting from loss of Pvr. This could suggest that the Pvr signaling is performing multiple

functions during WC and there is a split in the cascade downstream of the receptor (between Pvr/Ras and Mask/MKK3).

Interestingly, the Pvr suppressors found to be required for hemocyte spreading only partially overlap with those found required for WC. This is perhaps not too surprising since WC is a collective cell migration orchestrated by an epithelial tissue whereas hemocyte spreading is an individual change in morphology occurring in mesodermal cells. Control of actin dynamics is likely relevant in both of these tissues as Pvr has well-established roles in directing actin polymerization when overexpressed (Rosin et al. 2004) and during border cell migration (Poukkula et al. 2011). In summary, Akt is uniquely required for spreading *in vitro*; MKK3, Ras and Ck1 $\alpha$  are only required for epidermal WC; and Mask is required for both *in vitro* and *in vivo* spreading and WC. These results suggest the signaling cascade downstream of Pvr differs in the two cell types and it will be interesting, now that genes are identified, to probe how these differences interact with the cytoskeletal architecture to achieve the observed changes in cell morphology.

## Data availability

Strains and plasmids are available upon request. A Supplementary material file in the online of this article contains Supplementary Figures S1–S4 and Tables S1 (genotypes used in each figure) and S2 (genes screened in lethality suppressor screen). Supplementary Material is available at figshare: <https://doi.org/10.25387/g3.14758572>.

## Acknowledgments

We thank Drs Daniel Babcock and Amanda Brock for early work on wound-induced inflammation in our lab, Dr Adriana Paulucci-Holthausen and the MDA Department of Genetics microscopy facility for light microscopy assistance and Kenneth Dunner at the UT MD Anderson High Resolution Electron Microscopy Facility for electron microscopy assistance. Drs Swathi Arur, George Eisenhoffer, and Galko laboratory members read and commented on the manuscript.

## Funding

Work in the Galko lab was supported through a “people not projects” mechanism: R35GM126929 of the National Institute of General Medical Sciences (NIGMS). C.-R.T. was supported by an American Heart Association (AHA) predoctoral fellowship (16PRE30880004). A.J., N.S., and J.D.C. were supported by the Cancer Prevention and Research Institute of Texas (CPRIT) CURE Summer Undergraduate Research Training Program at MD Anderson Cancer Center (RP170067).

## Conflicts of interest

The authors declare that there is no conflict of interest.

## Literature cited

Adachi-Yamada T, Nakamura M, Irie K, Tomoyasu Y, Sano Y, et al. 1999. P38 mitogen-activated protein kinase can be involved in transforming growth factor beta superfamily signal transduction in *Drosophila* wing morphogenesis. *Mol Cell Biol.* 19:2322–2329.

Babcock DT, Brock AR, Fish GS, Wang Y, Perrin L, et al. 2008. Circulating blood cells function as a surveillance system for damaged tissue in *Drosophila* larvae. *Proc Natl Acad Sci U S A.* 105:10017–10022.

Baek SH, Kwon YC, Lee H, Choe KM. 2010. Rho-family small GTPases are required for cell polarization and directional sensing in *Drosophila* wound healing. *Biochem Biophys Res Commun.* 394:488–492.

Beinert N, Werner M, Dowe G, Chung HR, Jäckle H, et al. 2004. Systematic gene targeting on the x chromosome of *Drosophila melanogaster*. *Chromosoma.* 113:271–275.

Brand AH, Perrimon N. 1993. Targeted gene expression as a means of altering cell fates and generating dominant phenotypes. *Development.* 118:401–415.

Bretscher AJ, Honti V, Binggeli O, Burri O, Poidevin M, et al. 2015. The nimrod transmembrane receptor eater is required for hemocyte attachment to the sessile compartment in *Drosophila melanogaster*. *Biol Open.* 4:355–363.

Brock AR, Babcock DT, Galko MJ. 2008. Active cop, passive cop: developmental stage-specific modes of wound-induced blood cell recruitment in *Drosophila*. *Fly.* 2:303–305.

Brock AR, Wang Y, Berger S, Renkawitz-Pohl R, Han VC, et al. 2012. Transcriptional regulation of profilin during wound closure in *Drosophila* larvae. *J Cell Sci.* 125:5667–5676.

Bruckner K, Kockel L, Duchek P, Luque CM, Rorth P, et al. 2004. The PDGF/VEGF receptor controls blood cell survival in *Drosophila*. *Dev Cell.* 7:73–84.

Burra S, Wang Y, Brock AR, Galko MJ. 2013. Using *Drosophila* larvae to study epidermal wound closure and inflammation. *Methods Mol Biol.* 1037:449–461.

Cho NK, Keyes L, Johnson E, Heller J, Ryner L, et al. 2002. Developmental control of blood cell migration by the *Drosophila* VEGF pathway. *Cell.* 108:865–876.

D'Ambrosio MV, Vale RD. 2010. A whole genome RNAi screen of *Drosophila* S2 cell spreading performed using automated computational image analysis. *J Cell Biol.* 191:471–478.

Dietzl G, Chen D, Schnorrer F, Su KC, Barinova Y, et al. 2007. A genome-wide transgenic RNAi library for conditional gene inactivation in *Drosophila*. *Nature.* 448:151–156.

Duchek P, Somogyi K, Jekely G, Beccari S, Rorth P. 2001. Guidance of cell migration by the *Drosophila* PDGF/VEGF receptor. *Cell.* 107:17–26.

Eming SA, Krieg T, Davidson JM. 2007. Inflammation in wound repair: molecular and cellular mechanisms. *J Invest Dermatol.* 127:514–525.

Fernández-Espartero CH, Ramel D, Farago M, Malartre M, Luque CM, et al. 2013. GTP exchange factor Vav regulates guided cell migration by coupling guidance receptor signalling to local Rac activation. *J Cell Sci.* 126:2285–2293.

Friedman A, Perrimon N. 2006. A functional RNAi screen for regulators of receptor tyrosine kinase and Erk signalling. *Nature.* 444:230–234.

Galko MJ, Krasnow MA. 2004. Cellular and genetic analysis of wound healing in *Drosophila* larvae. *PLoS Biol.* 2:E239.

Garlena RA, Lennox AL, Baker LR, Parsons TE, Weinberg SM, Stronach BE. 2015. The receptor tyrosine kinase PVR promotes tissue closure by coordinating corpse removal and epidermal zipper. *Development.* 142:3403–3415.

Han C, Jan LY, Jan YN. 2011. Enhancer-driven membrane markers for analysis of nonautonomous mechanisms reveal neuron-glia interactions in *Drosophila*. *Proc Natl Acad Sci U S A.* 108:9673–9678.

- Han ZS, Enslin H, Hu X, Meng X, Wu IH, et al. 1998. A conserved p38 mitogen-activated protein kinase pathway regulates *Drosophila* immunity gene expression. *Mol Cell Biol.* 18:3527–3539.
- Harris KE, Schnitke N, Beckendorf SK. 2007. Two ligands signal through the *Drosophila* PDGF/VEGF receptor to ensure proper salivary gland positioning. *Mech Dev.* 124:441–448.
- Hatan M, Shinder V, Israeli D, Schnorrer F, Volk T. 2011. The *Drosophila* blood brain barrier is maintained by GPCR-dependent dynamic actin structures. *J Cell Biol.* 192:307–319.
- Heino TI, Karpanen T, Wahlstrom G, Pulkkinen M, Eriksson U, et al. 2001. The *Drosophila* VEGF receptor homolog is expressed in hemocytes. *Mech Dev.* 109:69–77.
- Ishimaru S, Ueda R, Hinohara Y, Ohtani M, Hanafusa H. 2004. Pvr plays a critical role via Jnk activation in thorax closure during *Drosophila* metamorphosis. *EMBO J.* 23:3984–3994.
- Janssens K, Sung HH, Rorth P. 2010. Direct detection of guidance receptor activity during border cell migration. *Proc Natl Acad Sci U S A.* 107:7323–7328.
- Jékely G, Sung HH, Luque CM, Rørth P. 2005. Regulators of endocytosis maintain localized receptor tyrosine kinase signaling in guided migration. *Dev Cell.* 9:197–207.
- Kadandale P, Stender JD, Glass CK, Kiger AA. 2010. Conserved role for autophagy in rho1-mediated cortical remodeling and blood cell recruitment. *Proc Natl Acad Sci U S A.* 107:10502–10507.
- Kakanj P, Moussian B, Gronke S, Bustos V, Eming SA, et al. 2016. Insulin and tor signal in parallel through FOXO and S6K to promote epithelial wound healing. *Nat Commun.* 7:12972.
- Karim FD, Rubin GM. 1998. Ectopic expression of activated ras1 induces hyperplastic growth and increased cell death in *Drosophila* imaginal tissues. *Development.* 125:1–9.
- Kiger AA, Baum B, Jones S, Jones MR, Coulson A, et al. 2003. A functional genomic analysis of cell morphology using RNA interference. *J Biol.* 2:27.
- Kim SN, Jeibmann A, Halama K, Witte HT, Wälte M, et al. 2014. ECM stiffness regulates glial migration in *Drosophila* and mammalian glioma models. *Development.* 141:3233–3242.
- Lawrence PA, Bodmer R, Vincent JP. 1995. Segmental patterning of heart precursors in *Drosophila*. *Development.* 121:4303–4308.
- Lee CW, Kwon YC, Lee Y, Park MY, Choe KM. 2019. Cdc37 is essential for Jnk pathway activation and wound closure in *Drosophila*. *Mol Biol Cell.* 30:2651–2658.
- Lee JH, Lee CW, Park SH, Choe KM. 2017. Spatiotemporal regulation of cell fusion by Jnk and Jak/stat signaling during *drosophila* wound healing. *J Cell Sci.* 130:1917–1928.
- Lee T, Feig L, Montell DJ. 1996. Two distinct roles for Ras in a developmentally regulated cell migration. *Development.* 122:409–418.
- Lesch C, Jo J, Wu Y, Fish GS, Galko MJ. 2010. A targeted UAS-RNAi screen in *Drosophila* larvae identifies wound closure genes regulating distinct cellular processes. *Genetics.* 186:943–957.
- Levin DM, Breuer LN, Zhuang S, Anderson SA, Nardi JB, Kanost MR. 2005. A hemocyte-specific integrin required for hemocytic encapsulation in the tobacco hornworm, *Manduca sexta*. *Insect Biochem Mol Biol.* 35:369–380.
- Lopez-Bellido R, Puig S, Huang PJ, Tsai CR, Turner HN, et al. 2019. Growth factor signaling regulates mechanical nociception in flies and vertebrates. *J Neurosci.* 39:6012–6030.
- McDonald JA, Pinheiro EM, Montell DJ. 2003. Pvf1, a PDGF/VEGF homolog, is sufficient to guide border cells and interacts genetically with Taiman. *Development.* 130:3469–3478.
- McGuire SE, Mao Z, Davis RL. 2004. Spatiotemporal gene expression targeting with the target and gene-switch systems in *Drosophila*. *Sci STKE.* 2004:pl6.
- Mondal BC, Shim J, Evans CJ, Banerjee U. 2014. Pvr expression regulators in equilibrium signal control and maintenance of *drosophila* blood progenitors. *Elife* 3:e03626.
- Moreira CG, Regan JC, Zaidman-Rémy A, Jacinto A, Prag S. 2011. *Drosophila* hemocyte migration: an in vivo assay for directional cell migration. *Methods Mol Biol.* 769:249–260.
- Moreira S, Stramer B, Evans I, Wood W, Martin P. 2010. Prioritization of competing damage and developmental signals by migrating macrophages in the *Drosophila* embryo. *Curr Biol.* 20:464–470.
- Munier AI, Doucet D, Perrodou E, Zachary D, Meister M, et al. 2002. Pvf2, a PDGF/VEGF-like growth factor, induces hemocyte proliferation in *Drosophila* larvae. *EMBO Rep.* 3:1195–1200.
- Nardi JB, Pilas B, Bee CM, Zhuang S, Garsha K, et al. 2006. Neuroglian-positive plasmatocytes of *Manduca sexta* and the initiation of hemocyte attachment to foreign surfaces. *Dev Comp Immunol.* 30:447–462.
- Ni JQ, Zhou R, Czech B, Liu LP, Holderbaum L, et al. 2011. A genome-scale shRNA resource for transgenic RNAi in *Drosophila*. *Nat Methods.* 8:405–407.
- Parsons B, Foley E. 2013. The *Drosophila* platelet-derived growth factor and vascular endothelial growth factor-receptor related (Pvr) protein ligands Pvf2 and Pvf3 control hemocyte viability and invasive migration. *J Biol Chem.* 288:20173–20183.
- Pastor-Pareja JC, Wu M, Xu T. 2008. An innate immune response of blood cells to tumors and tissue damage in *Drosophila*. *Dis Model Mech.* 1:144–154; discussion 153.
- Poukkula M, Cliffe A, Changede R, Rørth P. 2011. Cell behaviors regulated by guidance cues in collective migration of border cells. *J Cell Biol.* 192:513–524.
- Ramos-Lewis W, LaFever KS, Page-McCaw A. 2018. A scar-like lesion is apparent in basement membrane after wound repair in vivo. *Matrix Biol.* 74:101–120.
- Ratheesh A, Belyaeva V, Siekhaus DE. 2015. *Drosophila* immune cell migration and adhesion during embryonic development and larval immune responses. *Curr Opin Cell Biol.* 36:71–79.
- Ratheesh A, Biebl J, Vesela J, Smutny M, Pappusheva E, et al. 2018. *Drosophila* TNF modulates tissue tension in the embryo to facilitate macrophage invasive migration. *Dev Cell.* 45:331–346.e7.
- Rosin D, Schejter E, Volk T, Shilo BZ. 2004. Apical accumulation of the *Drosophila* PDGF/VEGF receptor ligands provides a mechanism for triggering localized actin polymerization. *Development.* 131:1939–1948.
- Russo J, Dupas S, Frey F, Carton Y, Brehelin M. 1996. Insect immunity: early events in the encapsulation process of parasitoid (*Leptopilina boulardi*) eggs in resistant and susceptible strains of *drosophila*. *Parasitology.* 112:135–142.
- Sinenko SA, Mathey-Prevot B. 2004. Increased expression of *Drosophila* tetraspanin, Tsp68C, suppresses the abnormal proliferation of ytr-deficient and Ras/Raf-activated hemocytes. *Oncogene.* 23:9120–9128.
- Smith RK, Carroll PM, Allard JD, Simon MA. 2002. Mask, a large ankyrin repeat and KH domain-containing protein involved in *drosophila* receptor tyrosine kinase signaling. *Development.* 129:71–82.
- Sopko R, Lin YB, Makhijani K, Alexander B, Perrimon N, et al. 2015. A systems-level interrogation identifies regulators of *drosophila* blood cell number and survival. *PLoS Genet.* 11:e1005056.
- Stramer B, Wood W, Galko MJ, Redd MJ, Jacinto A, et al. 2005. Live imaging of wound inflammation in *Drosophila* embryos reveals key roles for small GTPases during in vivo cell migration. *J Cell Biol.* 168:567–573.
- Stramer BM, Dionne MS. 2014. Unraveling tissue repair immune responses in flies. *Semin Immunol.* 26:310–314.

- Sullivan KM, Rubin GM. 2002. The  $Ca^{2+}$ -calmodulin-activated protein phosphatase calcineurin negatively regulates EGF receptor signaling in *Drosophila* development. *Genetics*. 161:183–193.
- Tsai CR, Galko MJ. 2019. Casein kinase 1 $\alpha$  decreases beta-catenin levels at adherens junctions to facilitate wound closure in *Drosophila* larvae. *Development*. 146:dev175133. doi: 10.1242/dev.175133.
- Tsai CR, Wang Y, Galko MJ. 2018. Crawling wounded: molecular genetic insights into wound healing from *Drosophila* larvae. *Int J Dev Biol*. 62:479–489.
- Vef O, Cleppien D, Löffler T, Altenhein B, Technau GM. 2006. A new strategy for efficient in vivo screening of mutagenized *Drosophila* embryos. *Dev Genes Evol*. 216:105–108.
- Venken KJ, Schulze KL, Haelterman NA, Pan H, He Y, et al. 2011. Mimic: a highly versatile transposon insertion resource for engineering *Drosophila melanogaster* genes. *Nat Methods*. 8:737–743.
- Wang Y, Antunes M, Anderson AE, Kadmas JL, Jacinto A, et al. 2015. Integrin adhesions suppress syncytium formation in the *Drosophila* larval epidermis. *Curr Biol*. 25:2215–2227.
- Weavers H, Liepe J, Sim A, Wood W, Martin P, et al. 2016. Systems analysis of the dynamic inflammatory response to tissue damage reveals spatiotemporal properties of the wound attractant gradient. *Curr Biol*. 26:1975–1989.
- Williams MJ, Ando I, Hultmark D. 2005. *Drosophila melanogaster* Rac2 is necessary for a proper cellular immune response. *Genes Cells*. 10:813–823.
- Wood W, Faria C, Jacinto A. 2006. Distinct mechanisms regulate hemocyte chemotaxis during development and wound healing in *Drosophila melanogaster*. *J Cell Biol*. 173:405–416.
- Wu Y, Brock AR, Wang Y, Fujitani K, Ueda R, et al. 2009. A blood-borne PDGF/VEGF-like ligand initiates wound-induced epidermal cell migration in *Drosophila* larvae. *Curr Biol*. 19:1473–1477.
- Zettervall CJ, Anderl I, Williams MJ, Palmer R, Kurucz E, et al. 2004. A directed screen for genes involved in *Drosophila* blood cell activation. *Proc Natl Acad Sci U S A*. 101:14192–14197.

Communicating editor: A. Bashirullah